Background Signals in FOS Data: Cerenkov and Scattered Light

Michael R. Rosa[1,2]

Abstract

The composite background of particle induced Cerenkov light and of scattered light underlying FOS exposures is discussed. The particle background estimation in the current pipeline software is shown to be inadequate, underestimating the actual levels by 0.0025 to 0.017 counts/sec/diode. Scattered light affects blue and red targets, and scales with spectral type and target brightness. Over 400 exposures in the *HST* science data archive are used to characterize the individual components and to derive recipes for re-calibration.

I. Unwanted signals

The Faint Object Spectrograph is composed of single pass, low dispersion, broad wavelength range spectrometers with reflective optics, equipped with one-dimensional detectors covered with entrance windows (MgF_2 and fused silica on the blue and red side respectively). This combination makes the FOS susceptible for several sources of unwanted signal. Background counts caused by light entering the entrance aperture may stem from diffuse grating scatter, ghost images produced at optical surfaces and un-baffled reflections off structural elements from within the enclosure. Background counts due to the high energy particle flux in the *HST* orbit are due to Cerenkov light induced in the photocathode faceplates. Thermionic dark count rates in the detectors are of order 0.0003 cts/sec/diode (Beaver & Lyons 1992), at least an order of magnitude below the particle induced count rates.

To achieve the limiting performance of the FOS on astronomical targets, one must be able to correct for any of these unwanted signals. Because the detectors are one-dimensional, background signals are not normally recorded separately and simultaneously with the science data. A few FOS modes do, however, provide short regions in diode space that are virtually opaque to the dispersed target light. Best examples are G130H with the blue digicon and G190H with the red digicon, where the cut-off due to absorption of light in the faceplates leaves a section of approximately 50 diodes for “background only” recording. Science data taken in these modes can be used to investigate the various sources of unwanted signal under conditions typical to science exposures.

---

1. ST-ECF, ESO, Garching, Federal Republic of Germany.
2. Affiliated to the Astrophysics Division of ESA.

The situation in the G130H FOS/BLUE mode is sketched in Figure 1, where *B* denotes the composite background level, *P* the contribution by particle induced light and *S* the total signal *B* + *target* recorded at around 1550Å. In the following I summarize results on the characteristics of the "unwanted signals" as obtained from an analysis of more than 400 science target exposures in the *HST* archive. A more detailed description on the scattered light aspect has been given elsewhere (Rosa 1993a,b), and an extensive discussion of the particle background will be presented shortly (Rosa 1994).

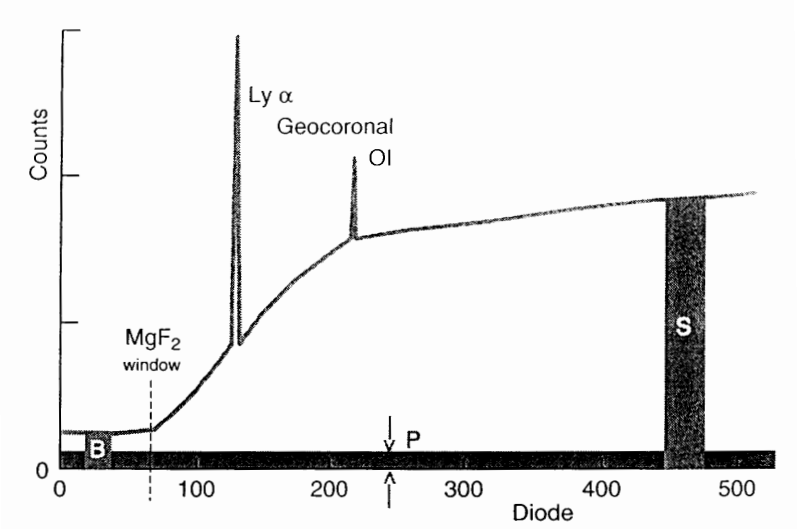

Figure 1: A sketch of raw data in diode space in G130 FOS/BLUE mode for a moderately bright blue target. Quantities obtained during the analysis of *HST* archive data are the average level *B* of composite background below the MgF_2 window cut-off, the average signal level *S*, including background, at around 1600Å, and the predicted particle induced background *P*.

II. Particle induced background

In-orbit dark measurements during OV/SV showed a mean background level of ≈ 0.007 cts/sec/diode in the blue detector and about 0.01 cts/sec/diode in the red side detector, i.e. a factor 30 above the pure thermionic noise. This background varies substantially with orbital parameters and time (Beaver & Lyons 1992, Lyons et al. 1992a). Important for the observer working on a particular data set are two aspects: the signal has a burst like character in time (showers of particles) and diode space (several diodes illuminated by one single event). The particle flux varies strongly ($\cos^4$ law) with the geomagnetic latitude of the spacecraft.

This has several effects on the data: The particle background in short duration exposures such as the default 4-8 min sub-exposures in a data set is very jagged and lumpy in diode space. Subtracting an average background value from a faint target signal therefore produces lots of negative residuals. Resampling algorithms that expect non-negative signal levels will therefore overestimate the observed flux. Data taken close to the extremes of geomagnetic latitude (+/– 40 degrees) suffer from about twice as much particle background as do data taken throughout the remaining 80 percent of the orbit. For really faint targets it may therefore be advantageous to inspect the individual groups and to exclude the few badly hurt sub-exposures from the final average taking.

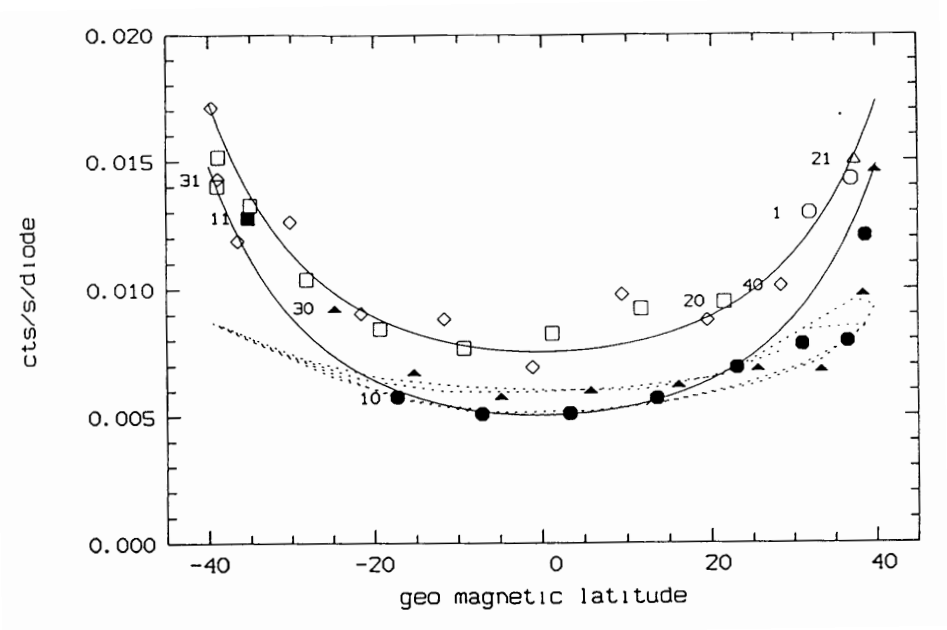

Figure 2: Particle induced background count rates as a function of geomagnetic latitude for 40 readouts covering two orbits. Filled symbols denote data taken in the dark parts of the orbit, open symbols data taken in the bright part of the orbit. The dashed line represents the pipeline prediction, the solid lines an empirical match of a $\cos^4$ type curve to the actual day/night side data.

The pipeline reduction, available off-line as CALFOS in STSDAS, incorporates a module that predicts the average particle background level, stores the prediction in the .c7h file and subtracts the estimate from the data counts prior to flat fielding and conversion to flux. Currently, the software module determines a weighted geomagnetic position for each data readout and scales a background model according to a look-up table derived from dark observations spread over geomagnetic longitude and latitude. The background models are analytic fits to dark observations with the blue and the red digicon recorded during OV/SV (Beaver & Lyons 1992). However, analysis of the G130H FOS/BLUE data in the science archive that are not subject to excessive scattered light shows, that this estimate of the in-orbit background is always too low. The predictions fall short by 30 to 80 percent from the actual value determined in the first 50 diodes (see Section 4).

A close look at particle background values recorded in science exposures that cover two orbits with 40 successive 5 min readouts sheds more light onto the nature of the failure to predict the background accurately. For an observation away from any detectable target flux (target acquisition failure) Figure 2 shows the background signal averaged over the first 50 diodes as a function of geomagnetic latitude. Different symbols refer to the 4 data sets with 10 readouts that span 2 complete orbits. Labels identify the 1st and 10th readout, so that one can trace *HST*'s path twice through the geomagnetic latitude parameter space. Filled symbols correspond to the data taken on the dark side of the orbit, open symbols refer to the sunlit orbital phase.

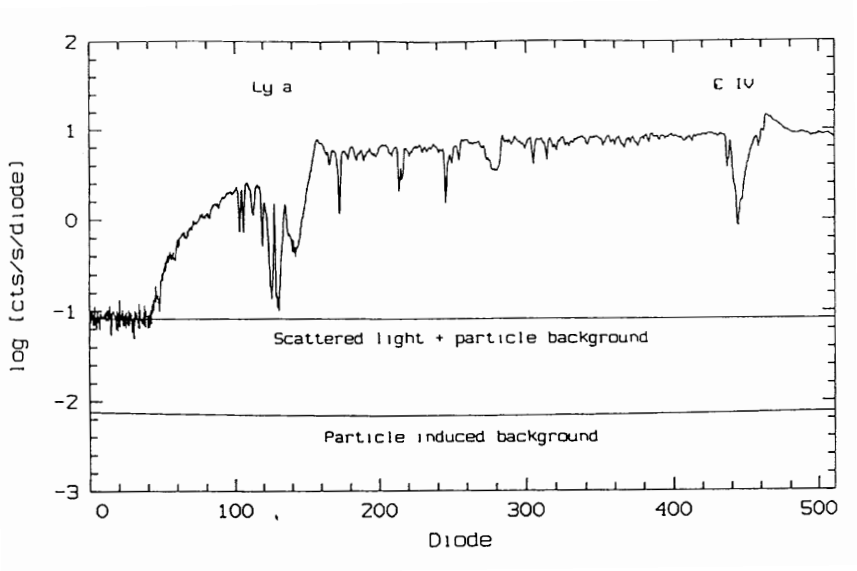

Figure 3: G130H FOS/BLUE spectrum of a bright O star with small interstellar reddening value. The signal drop-out at the entrance window cut-off (diode 50) can be clearly seen. Scattered light is about 10 times more important than Cerenkov light, and is responsible for about 50 percent of the residual intensity in the Lyα absorption trough.

The three curves show the prediction by the pipeline software (empirical scaling), and two modified versions of the $\cos^4$ function. The latter two test the hypotheses that (a) the scaling of the background in general needs to be revised upwards, and (b) the spacecraft travels through different particle flux densities in the compressed geomagnetic field facing the sun and the wake of the field downstream behind the earth. On the basis of observations dedicated to the detection of geocoronal, zodiacal and galactic background light (Lyons et al 1992b) it can be concluded that the diurnal variation seen here can not be due to solar stray light. Additional features not modeled properly are the bumps at 10 and 30 degree geomagnetic latitude, probably longitudinal variations due to the higher harmonics in the geomagnetic field. The present discussion indicates that a considerable improvement in the predictive power of the particle background module in the pipeline software can be expected if the current empirical scaling is superseded by a semi-empirical method incorporating geomagnetic field models.

III. Scattered light and ghosts

Pre-launch laboratory measurements using sequences of cut-on filters on Tungsten lamp illuminations of the apertures had shown a large susceptibility to diffuse scattered light in both blue and red channels (counts received in the wavelength range 1600Å to 2300Å (grating G190H) were almost entirely due to photons with effective wavelengths between 3500Å and 5500Å (Koornneef 1984, Sirk & Bohlin 1985) and see discussion by Kinney, this volume). Other indications for scattered light in the dispersion direction are found in anomalies of excess blue light reported by Lindler & Bohlin (1985) and Uomoto et al. (1989) from tests originally concerned with scattered light *perpendicular* to the dispersion direction.

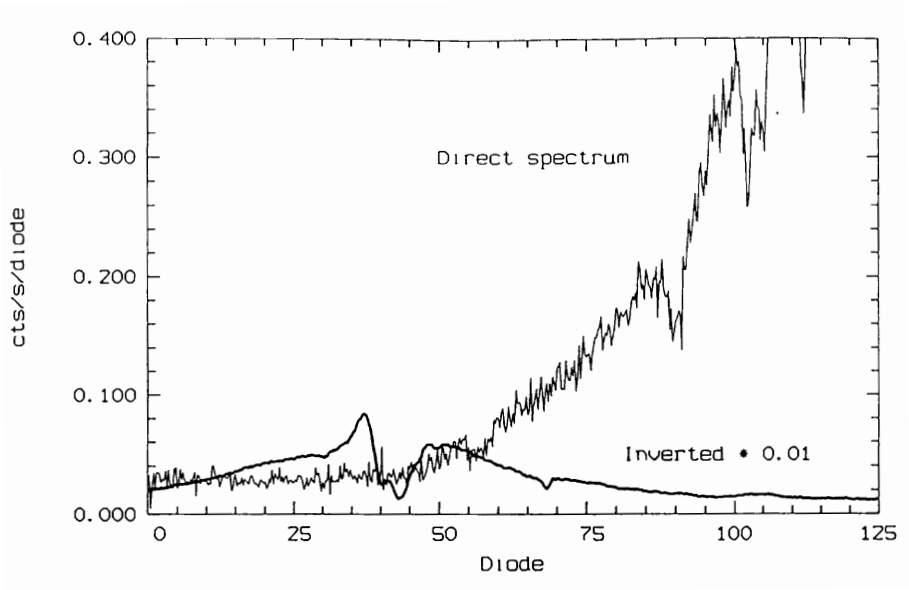

Figure 4: G130H FOS/Blue spectrum of an AGN (solid) with its mirror imaged version superimposed at 1/100th intensity (bold). If the mirror imaged C IV emission indeed produced a ghost image at around the MgF_2 window cut-off, its strength must be much less than 0.01 the intrinsic C IV counts.

How large are the effects on science data taken with FOS? Although tests with non-astronomical light sources are able to generate the majority of calibration data, only the analysis of data of real astronomical sources with presumably well known spectra can show whether all adverse effects are under control. One can identify three categories of targets – critical in terms of impact on the scientific data and informative in terms of a possible separation of the three suspected background sources – namely particle induced, grating scatter and ghosts.

Faint targets with blue spectra

If the count rates due to the intrinsic target spectrum are comparable to the in-orbit particle background rate of ≈0.007 cts/sec/diode, the determination of the intrinsic energy distribution critically depends upon the ability to correctly predict the actual background. For such faint blue targets any grating scatter and ghosts are much weaker than the particle background. Ideally, i.e. if the background model is fully applicable (see above), the ratio $R = B / P$ should then be unity.

Bright blue targets

The signal below 1150Å might consist of particle induced background and scattered light, likely from photons in the 3000Å to 5500Å range. A typical case is shown in Figure 3. Such targets might also produce detectable ghost spectra. One form of ghost images seen often in medium resolution ground based spectrographs equipped with CCD dewars with flat entrance windows is a mirror imaged spectrum of about 1/100 to 1/1000 the intensity of the primary spectrum, the location of the center of

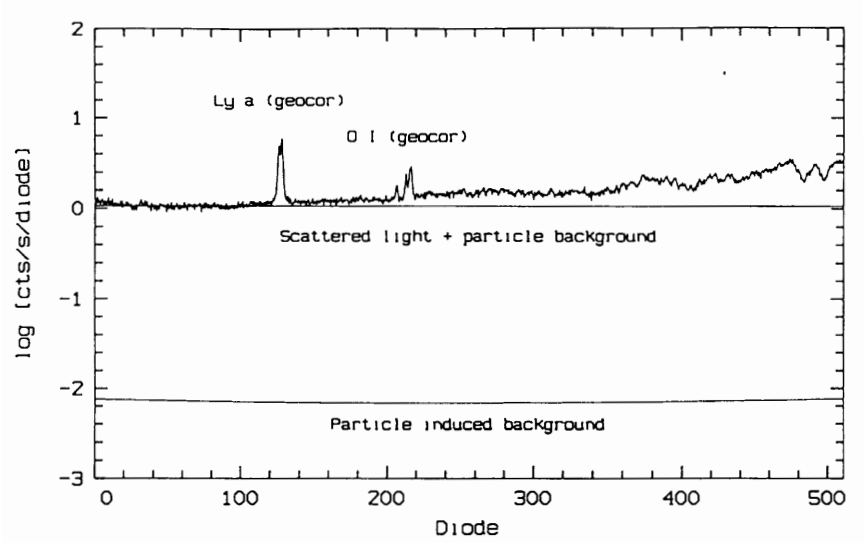

Figure 5: G130 FOS/BLUE spectrum of a solar-type star. Scattered light (assumed to be constant in diode space) is 100 times more important than Cerenkov light, and dominates the signal throughout most of the spectral range.

symmetry depending on the alignment of the detector surface and the window surface.

This type of ghost can be tested for in the spectrum of an AGN with appreciable redshift as displayed in Figure 4 together with a mirror image at 1/100 intensity. No ghost images can be seen of either the C IV or the geocoronal Lyman α or O I lines. On the basis of this and similar data it seems unlikely that mirror imaged ghost spectra are present at light levels ≥1/500 the illuminating intensity in mode FOS BLUE, G130H. The same is true for mode FOS RED, G780H where the Hα emission line can be used for this purpose.

Red targets with intrinsically faint blue spectra

The signal shortward of 1150Å will be composed of the actual particle induced background as discussed above plus grating scattered photons from the 3000Å to 5500Å domain. For intrinsically bright red targets the latter component is overwhelming. Figure 5 shows an example of this target class – here a solar type star. The scattered light is the dominant background source. Since this background can only be assessed in the first 50 diodes, its actual shape remains unknown. Only inter-instrument comparison of GHRS and FOS data on the same star and/or a comparison with predicted data using stellar atmosphere models and interstellar extinction laws can give more insight (see the contributions by A. Kinney and J. Caldwell in this volume).

IV. An empirical model of the unwanted signals

The examples have shown two significant contributors to the background level observed in the FOS BLUE, G130H mode. On the one hand the anticipated particle induced Cerenkov light is at levels in excess of the predictions from the model used in

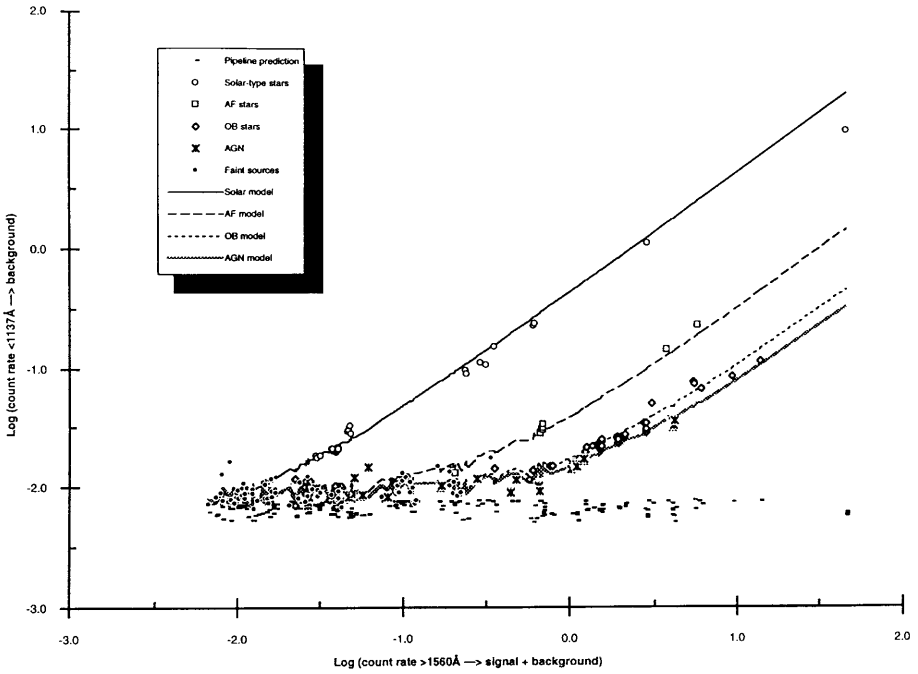

Figure 6: Background versus signal diagram for G130H FOS/BLUE mode science observations of various classes of targets. Refer to Figure 1 for definitions. Dashes show the predicted particle background for each of the data points included. Solid lines are the empirical models for each target class as described in the text.

the standard data calibration pipeline. On the other hand, there is grating scatter, presumably of light from the spectral range 3000Å to 5500Å. This is again evidenced, now for the full sample of relevant science data in the *HST* archive, in Figure 6. On a logarithmic scale are shown the values B (measured background below 1137Å) versus S (measured signal + background above 1560Å), grouped into different target categories (see legend). Also shown by small dots are the values of the background predicted in the pipeline reduction P versus S.

Faint and very faint targets (open circles) are found at count rates below 0.3 cts/s/diode or $\log(S) \leq -0.5$. As can be seen, all measurements of the background level, even those for the faintest targets are larger than the predicted ones. For targets with appreciable flux at wavelengths above 1560Å, B is a nearly linear function of S, with scale coefficients depending on target type – very red solar type spectra, A type stars, OB type stars and AGNs can be easily distinguished. This is clear evidence for grating scatter of photons at wavelengths outside the range imaged by the G130H grating. The tight relations do suggest that correction formulae can be derived if the spectral energy distribution in the wavelength range from 1600Å to 5500Å is known. Further, the faint target data – i.e. B dominated by P – show that the background model in use in the pipeline underestimates the absolute level by a factor 1.3 to 1.8.

An empirical model matching the data of bright targets – i.e. S/P large – and providing a lower limit to the very faint target data has the form:

$$b = g \times P + (S - g \times P) \times f$$

where b is an estimate of B at 1100Å; g is the gain factor for the pipeline predicted particle background P; S is the total signal at 1600Å; and f is a scale factor for scattered light.

The gain factor for the particle background predicted by the current pipeline software is $1.3 < g < 1.8$. Scattered light scale factors f as determined from the data in Figure 4 are: 0.44 ± 0.09 (G, K, M stars and solar system bodies); 0.032 ± 0.006 (A, F stars); 0.010 ± 0.002 (O, B stars); and 0.007 ± 0.001 (various AGNs).

The low value of f for AGNs presumably reflects the fact that the wavelength range used to determine S incorporates the redshifted C IV emission line. Given that no individual corrections for interstellar extinction have been made, and that targets have been assigned to very loosely defined groupings, the tightness of the relations found is astonishing. This fact also argues in favor of a diffuse scattering mechanism against ghost images where spectral features differ from one target to the next even within one grouping.

V. Removal of unwanted signal in G130 FOS/BLUE mode

As a result, the level of unwanted signal in FOS BLUE, G130H mode observations in the first 50 diodes can be predicted successfully by scaling the pipeline prediction of the particle background and adding a component due to scattered light which scales with spectral type and target brightness at 1600Å. The present analysis cannot answer the question of whether or not the scattered light component is constant across the detector.

Assuming that this is a good zero order estimate, and noting that the particle background is nearly constant across the detector, the unwanted signal as a function of location on the detector can than empirically be estimated for each individual exposure with sufficient accuracy by the following formula:

$$b(diode) = 1.3 \times P(diode) + q;\ b(1\ to\ 45) = B(1\ to\ 45)$$

where q is a constant used to match the observed level below 1037Å and corrects for a constant level of scattered light.

For those GOs not having direct access to the STSDAS FOS package and the CDBS calibration reference files, the re-calibration of data can be performed according to the relations

$$new\ back = 1.3 \times old\ back + q$$
$$flat = flatfielded\ counts / (counts - old\ back)$$
$$inverse\ sensitivity = old\ flux / (flatfielded\ counts)$$
$$new\ flux = (counts - new\ back) \times flat \times inverse\ sensitivity$$

where the input data are in files .c1h (old flux); .c4h (counts); .c5h (flatfielded counts) and .c7h (old back).

Presumably the factor g = 1.3 is valid for other grating combinations with the blue detector. For faint targets allowance for a scale factor in the particle background alone could probably be adequate. However, the amount of scattering in these modes (G190H, G270H etc.) is not known and cannot be assessed directly in the way done here for G130H. A preliminary result of g ~ 1.3 has also been found for FOS RED, G780H, using only a small database however.

References

Beaver, E.A., & Lyons, R.W., 1992, Instrument Science Report CAL/FOS–076, STScI
Koornneef, J., 1984, Instrument Science Report CAL/FOS–005, STScI
Lindler, D., & Bohlin, R., 1985, Instrument Science Report CAL/FOS–011, STScI
Lyons, R.W., Baity, W., Beaver, E.A., Cohen, R.D., Junkkarinen, V.T., Linsky, J.B., & Rosenblatt, E.I., 1992a, Instrument Science Report CAL/FOS–080, STScI
Lyons, R.W., Baity, W., Beaver, E.A., Cohen, R.D., Junkkarinen, V.T., & Linsky, J.B., 1992b, Instrument Science Report CAL/FOS–083, STScI
Rosa, M.R., 1993a, ST–ECF Newsletter, 20, 14
Rosa, M.R., 1993b, Instrument Science Report CAL/FOS–113, STScI
Rosa, M.R., 1994, Instrument Science Report CAL/FOS, STScI
Sirk, M., & Bohlin, R., 1985, Instrument Science Report CAL/FOS–013, STScI
Uomoto, A., Blair, W.P., & Davidsen, A.F., 1989, Instrument Science Report CAL/FOS–059, STScI